

Na-decorated binary spinel ferrite catalysts for the hydrogenation of CO₂ to olefins

Hanjun Lu,¹ Xia Li,¹ Guangchao Li,^{2,*} Xinlin Hong^{1,*} Shik Chi Edman Tsang²

Methods

Synthesis of MFe₂O₄. The different transition metals spinel ferrite was prepared by an organic combustion method with the M/Fe atomic ratio of 1:2 (at/at) (M = Zn, Cu, Co). Typically, 16.16 g of Fe(NO₃)₃·9H₂O, 5.95 g of Zn(NO₃)₂·6H₂O and 23.06 g of citric acid monohydrate were dissolved in 23 mL of deionized water. The initial mixture was stirred to form a homogeneous aqueous solution and heated at 90 °C for 4 h. The obtained paste was then dried at 120 °C overnight.

Synthesis of Fe₂O₃. The Fe₂O₃ was prepared following the similar procedure. Typically, the 24.24 g of Fe(NO₃)₃·9H₂O and 23.06 g of citric acid monohydrate were dissolved in 23 mL of deionized water. The initial mixture was stirred to form a homogeneous aqueous solution and heated at 90 °C for 4 h. The obtained paste was then dried at 120 °C overnight.

Synthesis of NaMFe. The NaMFe catalyst was prepared by incipient wetness impregnation method. By controlling the impregnation content, the Na content in all catalysts is 2 wt%. Typically, the Fe₃O₄ powder was placed into 2 mL of Na₂CO₃ solution and kept for 2 h at room temperature under constant stirring, completely dried by rotary evaporation, and then calcined in the muffle oven at 400 °C for 4 h with a heating rate of 2 °C min⁻¹. The obtained different catalysts were labeled as NaMFe catalyst, where M represents the transition metal elements.

Synthesis of NaCoFe with different Fe/Co ratio. The NaCoFe with different Fe/Co ratio was prepared following the similar procedure as NaCoFe.

Catalytic testing. The evaluation of the catalyst was conducted in a fixed-bed reactor with an inside diameter of 6 mm. Firstly, 0.2 g precursor catalysts were mixed with 0.4 g quartz sand (40-60 mesh) and pre-reduced in a H₂ stream (30 mL min⁻¹) at 400 °C under atmospheric pressure for 2 h. After the temperature cooled down below 320 °C, a reactant (CO₂/H₂=1/3 by volume, 4 vol% N₂ as an internal standard, and GHSV of 3000 mL g_{cat}⁻¹ h⁻¹) was inducted into the reactor. Then the pressure and temperature were adjusted to the desired value (typically 1 MPa and 320 °C, respectively) to initiate the reaction. The reaction conditions were as follows except for those special labeled: H₂/CO₂ = 3; pressure, 1 MPa; temperature, 320 °C; and gas hourly space velocity (GHSV), 3000 mL g_{cat}⁻¹ h⁻¹. The products were monitored online by a gas chromatograph equipped with a thermal conductivity detector (TCD, TDX-01 column) and flame ionization detector (FID, CB-Plot Q capillary column).

The CO₂ conversion, CO selectivity, C_i products selectivity and CO-free products selectivity were calculated according to the following equations 1-4:

$$\text{CO}_2 \text{ Conversion} = \frac{\text{CO}_2 \text{ in} - \text{CO}_2 \text{ out}}{\text{CO}_2 \text{ in}} \times 100\% \quad (\text{Eq 1})$$

$$\text{CO Selectivity} = \frac{\text{CO}_2 \text{ out}}{\text{CO}_2 \text{ in} - \text{CO}_2 \text{ out}} \times 100\% \quad (\text{Eq 2})$$

$$\text{C}_i \text{ Selectivity} = \frac{\text{C}_{i \text{ out}} \times i}{\text{CO}_2 \text{ in} - \text{CO}_2 \text{ out}} \times 100\% \quad (\text{Eq 3})$$

$$\text{CO free } C_i \text{ Selectivity} = \frac{C_{i \text{ out}} \times i}{\sum_{i=1}^n C_{i \text{ out}} \times i} \times 100\% \quad (\text{Eq 4})$$

Where $\text{CO}_{2 \text{ in}}$ and $\text{CO}_{2 \text{ out}}$ stand for moles of CO_2 at the inlet and outlet, respectively. CO_{out} refers to CO at the outlet. $C_{i \text{ out}}$ and i denote the carbon moles and carbon number of the carbon products (C_i) at the outlet. The catalytic results show that the carbon balance was close to within 5 %.

H₂-TPR measurements. Temperature-programmed reduction of H₂ (H₂-TPR) were measured by using a Micromeritics Autochem 2920. Typically, 30 mg of catalyst was placed into a U-type quartz tube and pre-treated in a high purity Ar gas (30 mL min⁻¹) at 150 °C for 1 h. After cooled down to room temperature, the gas was switched into 5 vol% H₂/Ar (30 mL min⁻¹) and the tube was purged for 10 min. After that, the sample temperature was ramped up to 900 °C with a heating rate of 10 °C min⁻¹, and a TCD (thermal conductivity detector) recording was simultaneously started.

CO₂-TPD measurements. Temperature-programmed desorption with CO₂ (CO₂-TPD) were done on Micromeritics AutoChem 2920 apparatus with an on-line Hiden QIC-20 mass spectrometer. Briefly, 30mg of catalyst was pretreated with 5 vol% H₂/Ar at 400 °C for 2 h and cooled to 50 °C. Afterwards, the pretreated catalyst was exposed to pure CO₂ at 50 °C for 30 min and then purged with Ar flow at the same temperature to eliminate all physisorbed CO₂. After 1 h purging, the temperature was raised from 50 to 800 °C (10 °C min⁻¹ ramp rate) as CO₂ desorption (m/z signal = 44) was monitored by mass spectrometer.

H₂-TPD measurements. Temperature-programmed desorption with (C₂H₄-TPD) were also measured using the same Micromeritics Autochem 2920 instrument and H₂ desorption (m/z signal = 2) was monitored by mass spectrometer. The procedures are similar to those employed for CO₂-TPD except that CO₂ was replaced with 5 vol% H₂/Ar.

C₂H₄-TPD measurements. Temperature-programmed desorption with (C₂H₄-TPD) were also measured using the same Micromeritics Autochem 2920 instrument and C₂H₄ desorption (m/z signal = 28) was monitored by mass spectrometer. The procedures are similar to those employed for CO₂-TPD except that CO₂ was replaced with 5 vol% C₂H₄/N₂.

C₂H₄-PTH measurements. Pulse transient hydrogenation with C₂H₄ (C₂H₄-PTH) were performed as follows: 30mg of spent catalyst was pretreated with 5 vol% H₂/Ar (30 mL min⁻¹) at 320 °C for 1 h. Afterwards, the C₂H₄ pulse was imported into the reactor for several cycles with an interval time of 10 min. The MS signals of C₂H₄ (m/z = 28) and C₂H₆ (m/z = 30) were collected.

Material characterization. XRD patterns were obtained on a Rigaku Miniflex600 (Japan) X-ray diffractometer with a Cu K α ($\lambda = 0.15406$ nm) radiation source. Brunauer-Emmett-Teller (BET) surface area and pore structure were analyzed on a Micromeritics ASAP-2020 automatic

N₂ adsorption system (America). The loading of Na and Zr was measured by inductively coupled plasma-atomic emission spectrometry (ICP-AES) on an IRIS Intrepid II XSP instrument. X-ray photoelectron spectra (XPS) were carried out on a Thermo Scientific ESCALAB 250Xi X-ray photoelectron spectrometer with a monochromatic Al K α source ($h\nu = 1486.6$ eV) with an operating power of 150 W (15 kV, 10 mA). Scanning electron microscope (SEM) studies were performed on an S-4800 instrument (Japan). Transmission electron microscopy (TEM) images, high-angle annular dark-field scanning TEM (HAADF-STEM), and energy-dispersive X-ray (EDX) mapping were recorded on a Tecnai G2 F30 S-TWIN electron microscope.

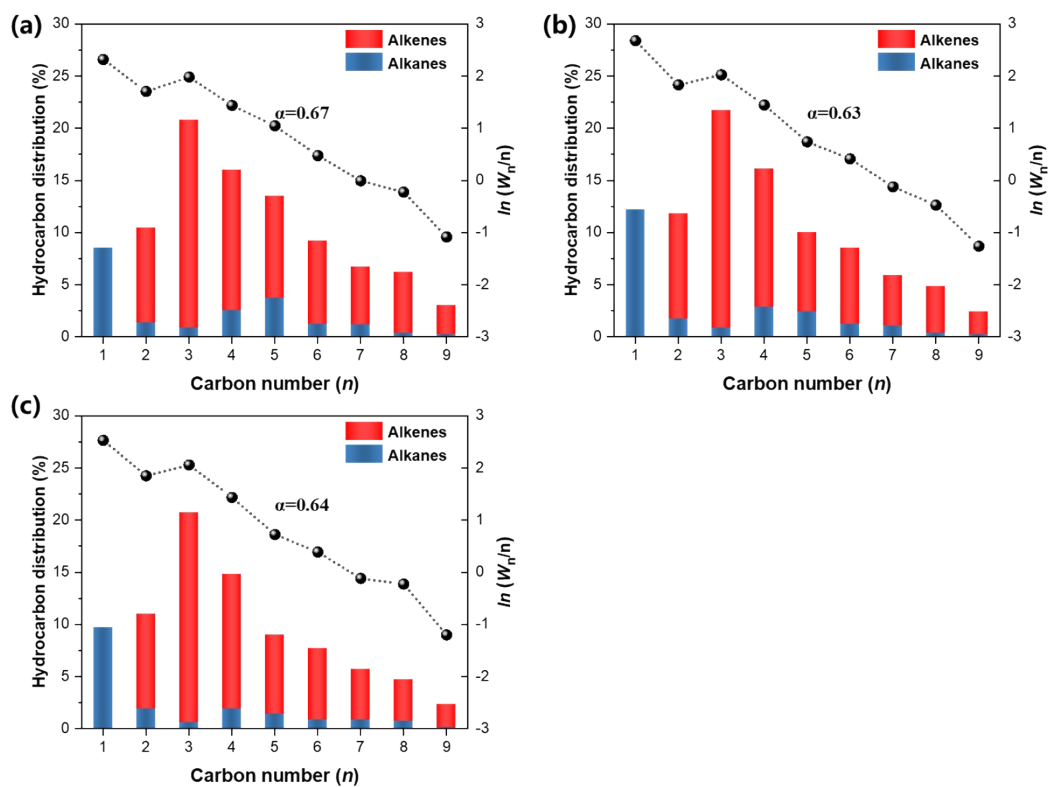


Figure S1. The detailed alkane and olefin distribution, the ASF plot and the corresponding α value (α represents the probability of chain growth) of (a) NaFe; (b) NaZnFe; (c) NaCuFe.

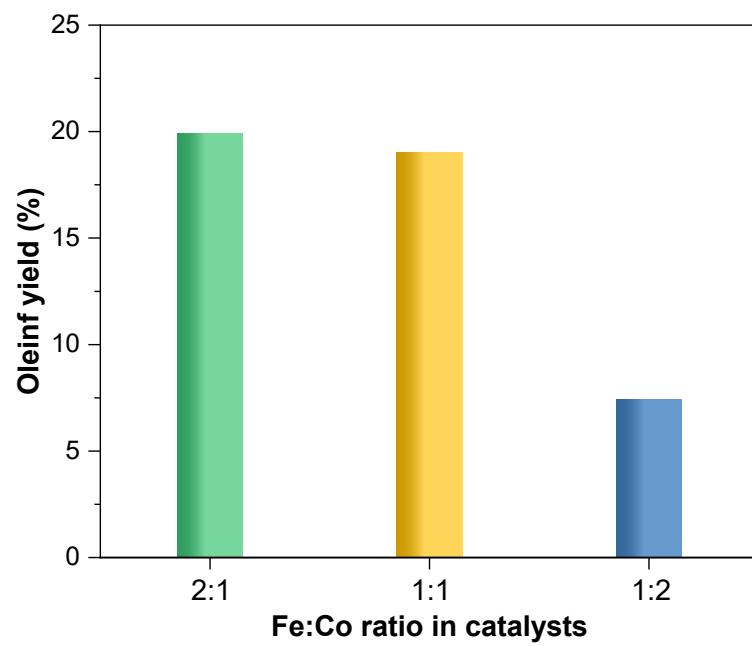


Figure S2. olefin yield over NaCoFe catalysts with different Fe:Co molar ratio.

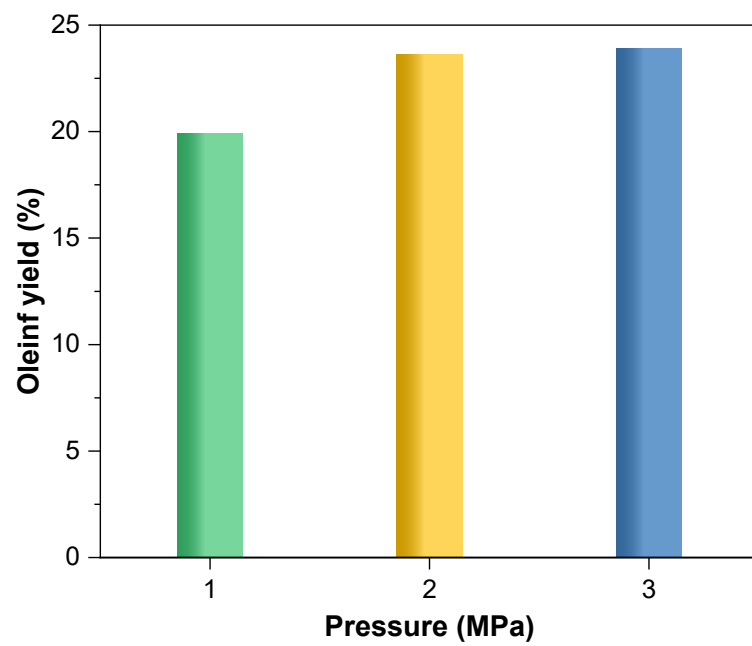


Figure S3. The effect of reaction pressure on the olefin yield.

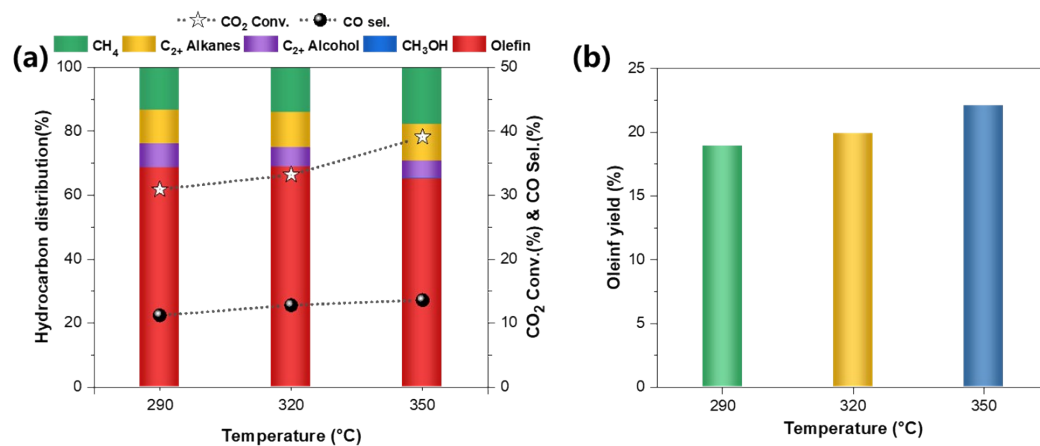


Figure S4. The effect of reaction temperature on the catalytic performance toward CO₂ hydrogenation. (a) The product distribution, CO₂ conversion, CO selectivity, and (b) olefin yield.

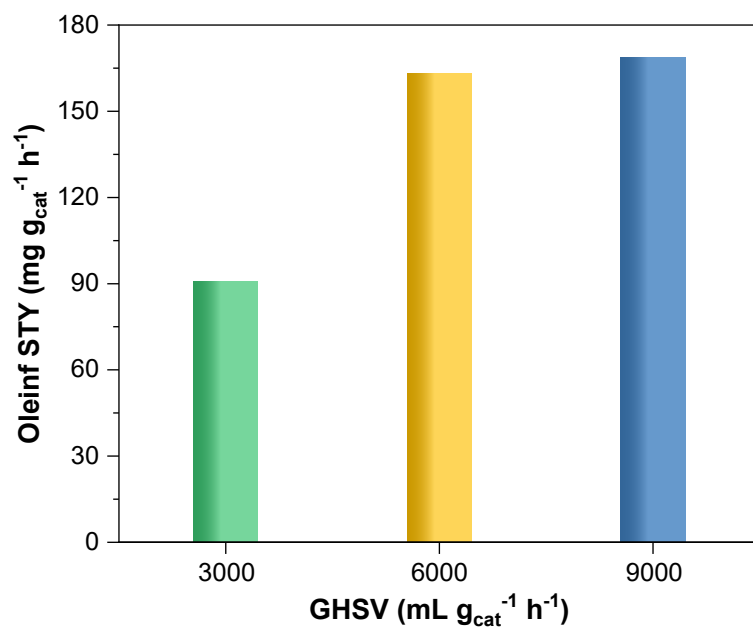


Figure S5. The effect of gas hourly space velocity (GHSV) on the STY of olefin.

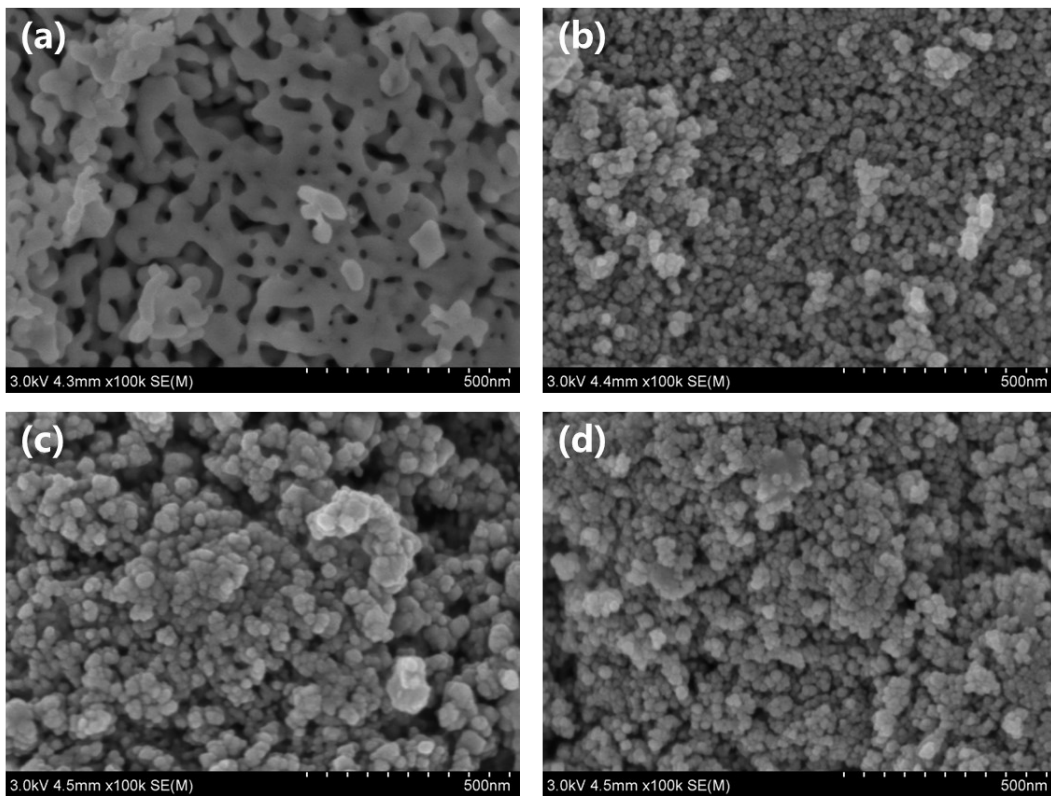


Figure S6. SEM images of fresh catalyst: (a) NaFe; (b) NaZnFe; (c) NaCuFe; (d) NaCoFe

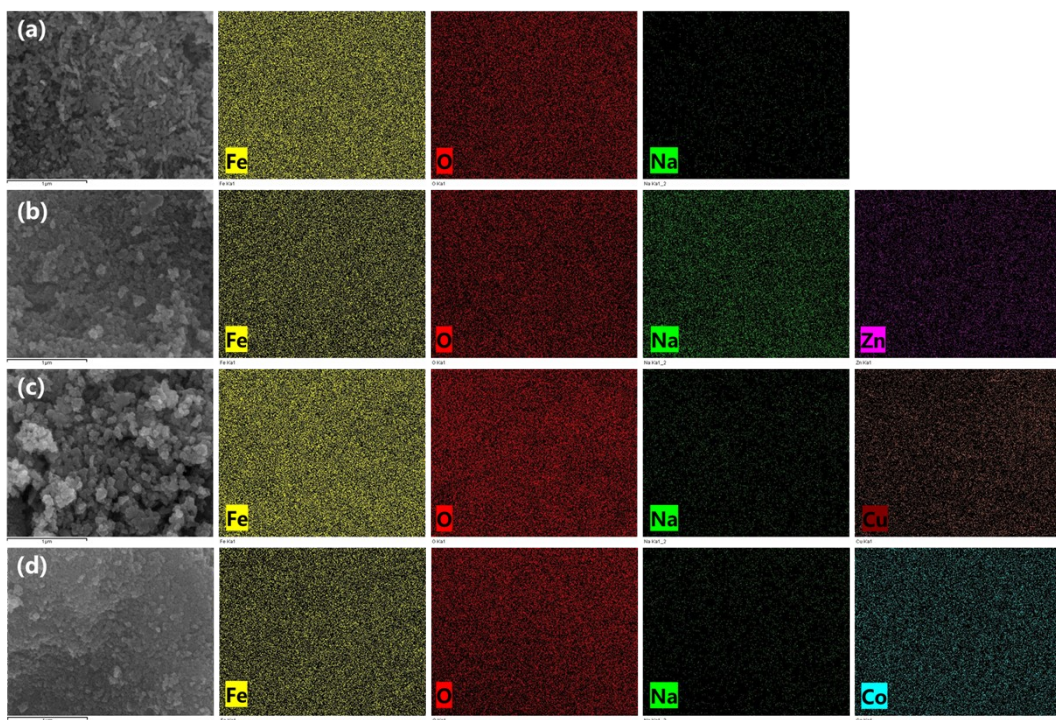


Figure S7. SEM images and elemental mapping images of (a) NaFe; (b) NaZnFe; (c) NaCuFe; (d) NaCoFe

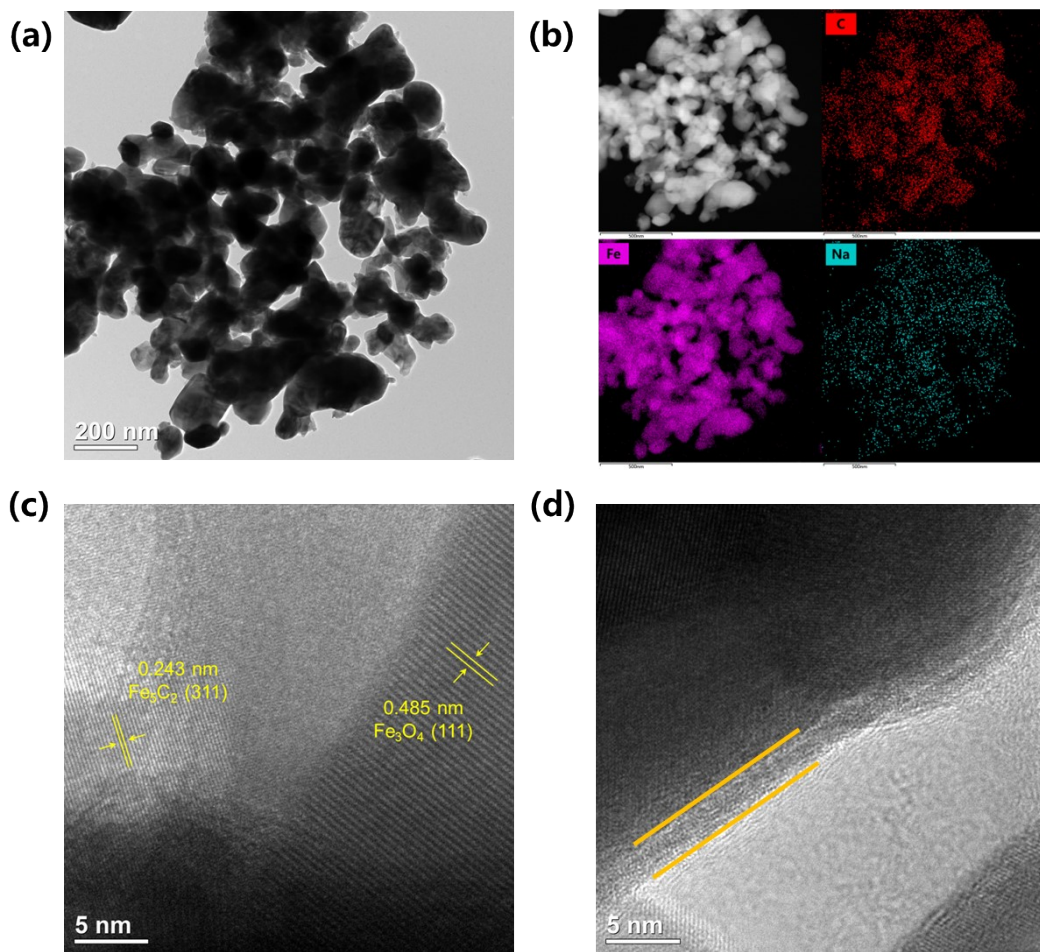


Figure S8. (a) TEM images; (b) STEM images with corresponding elemental mapping of Co, Fe, Na and (c, d) HRTEM images of the spent NaFe sample.

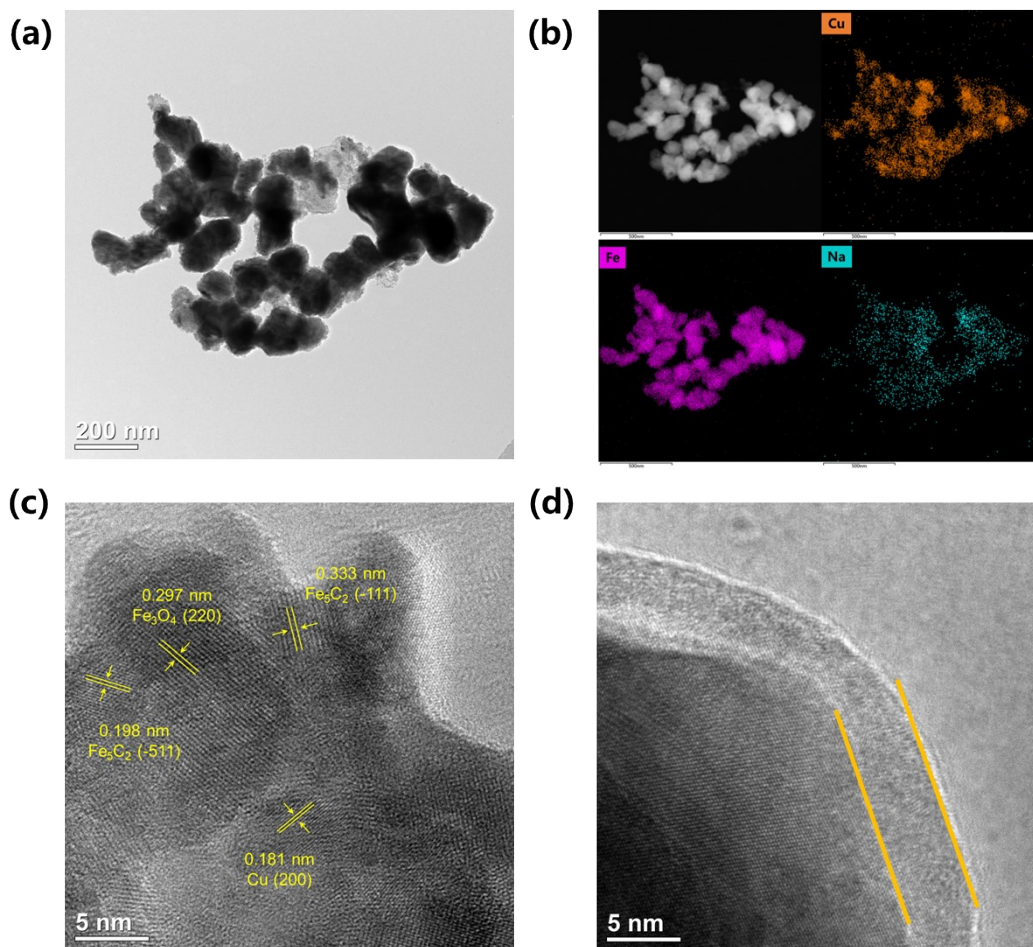


Figure S9. (a) TEM images; (b) STEM images with corresponding elemental mapping of Co, Fe, Na and (c, d) HRTEM images of the spent NaCuFe sample.

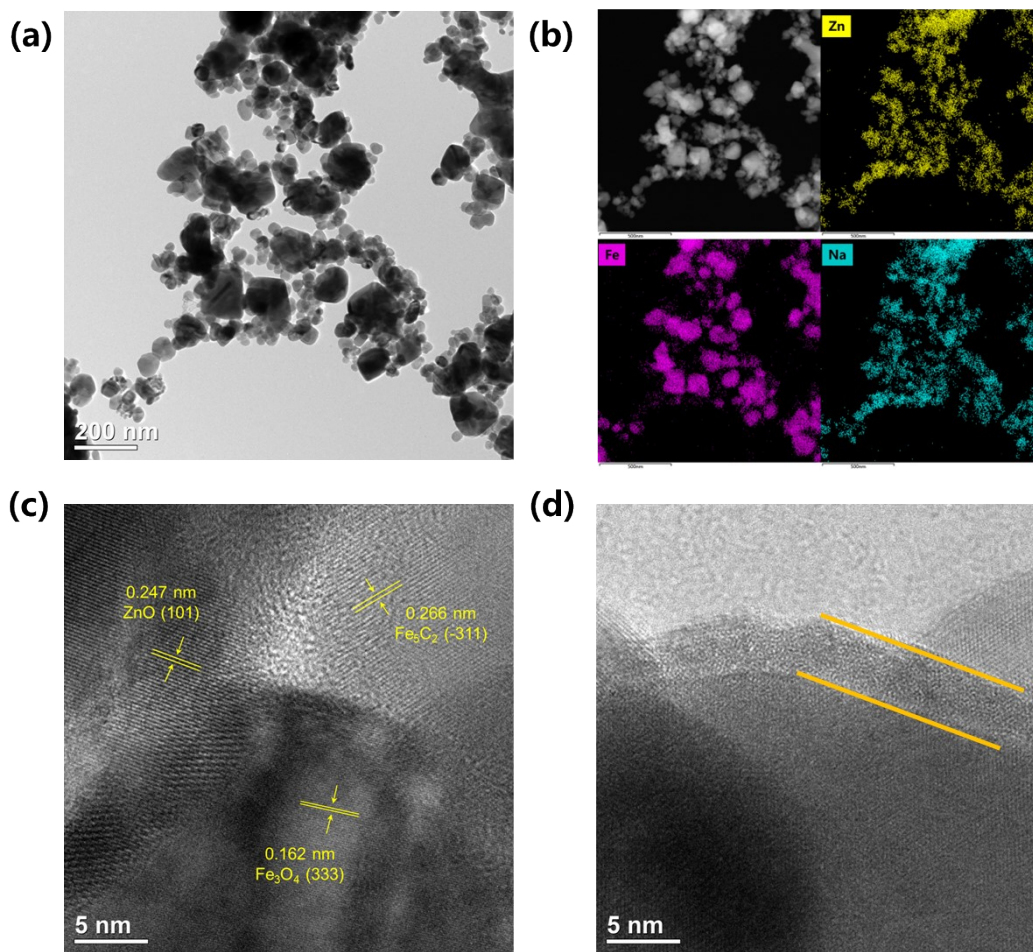


Figure S10. (a) TEM images; (b) STEM images with corresponding elemental mapping of Co, Fe, Na and (c, d) HRTEM images of the spent NaZnFe sample.

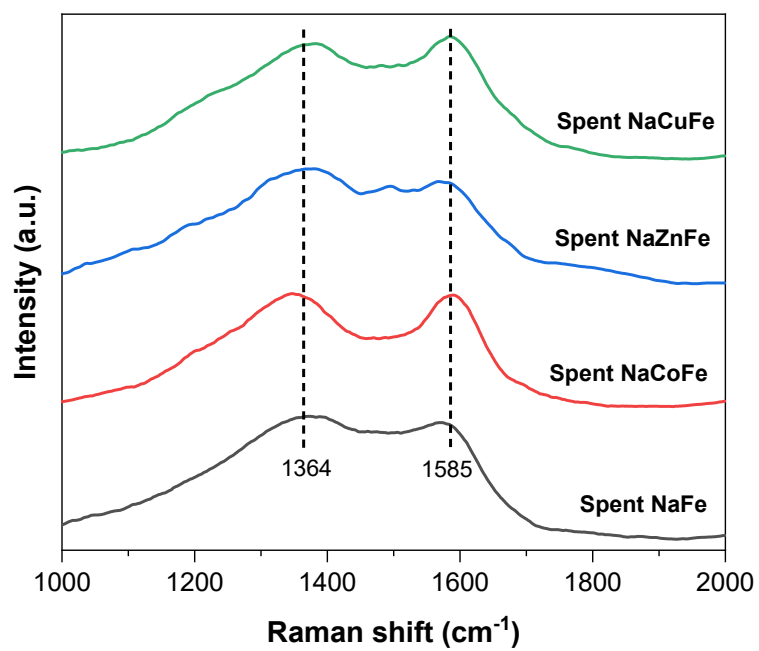


Figure S11. Raman spectra of the spent catalysts.

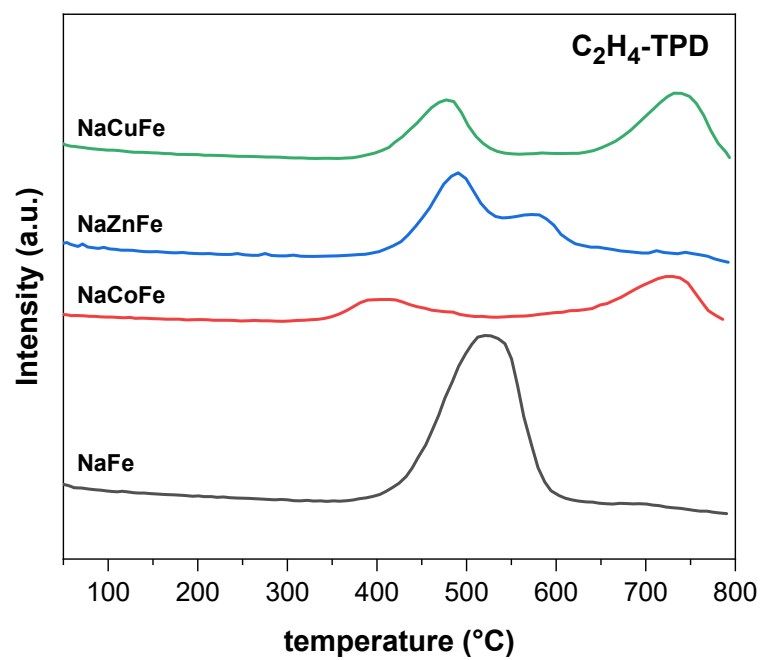


Figure S12. C₂H₄-TPD profiles of the Fe-based catalysts.

Table S1. Catalytic performance of Fe-based catalysts in CO₂ hydrogenation

Catalysts	CO ₂ Conv. (%)	CO Sel.(%)	CO-free Selectivity (%)				Olefin yield(%)
			CH ₄	C ₂₊ alkanes	C ₂₊ Alcohols	Olefin	
NaFe	27.7	16.8	8.5	11	5.7	74.8	17.2
NaZnFe	27.3	18.6	12.2	10.4	6.4	71	15.8
NaCuFe	27.8	18.4	9.7	8.3	13.4	68.4	14.6
NaCoFe	33.2	12.8	14.0	11.1	6.1	68.8	19.9